

Activation of the anaphase promoting complex by HTLV-1 tax leads to senescence

Yu-Liang Kuo and Chou-Zen Giam*

Department of Microbiology and Immunology, Uniformed Services University of the Health Sciences, Bethesda, MD, USA

The human T-lymphotropic virus type 1 (HTLV-1) Tax binds the anaphase promoting complex (APC) and activates it ahead of schedule. Here, we show that APC activation by Tax induces rapid senescence (*tax*-IRS) independently of p53 and pRB. In response to *tax*, cyclin A, cyclin B1, securin, and Skp2 becomes polyubiquitinated and degraded starting in S phase. This is followed by a surge in p21^{CIP1/WAF1} and p27^{KIP1} in mid to late S and G₂/M leading to a permanent G₁ arrest. Tax-positive HTLV-1-transformed T-cell lines express elevated levels of p21^{CIP1/WAF1}, but low levels of p27^{KIP1}. Finally, Tax can be stably expressed in p27^{KIP1}-null NIH3T3 cells. These results indicate that APC activation by Tax causes inactivation of SCF^{Skp2} and stabilization of p21^{CIP1/WAF1} and p27^{KIP1}. The build-up of p21^{CIP1/WAF1} and especially p27^{KIP1} commits cells to senescence. Evading *tax*-IRS through a loss of p27^{KIP1} function is likely to be critical for cell transformation by Tax and development of adult T-cell leukemia after HTLV-1 infection. Finally, activation of APC ahead of schedule may be exploited to arrest cancer cell growth.

The EMBO Journal advance online publication, 6 April 2006; doi:10.1038/sj.emboj.7601054

Subject Categories: cell cycle

Keywords: anaphase promoting complex; cyclin-dependent kinase inhibitor; HTLV-1 Tax; senescence; Skp1-Cullin-F-box

Introduction

Human T-lymphotropic virus type I (HTLV-1) is the etiological agent of adult T-cell leukemia/lymphoma (ATL) and a neurological disorder called HTLV-1-associated myelopathy/tropical spastic paraparesis (HAM/TSP). How HTLV-1 infection progresses to T-cell malignancy and HAM/TSP is not well understood but is thought to involve the viral transactivator/oncoprotein, Tax. The effects that Tax exerts on cells are pleiotropic, and include potent NF- κ B activation, cell cycle perturbation, and cell transformation. How Tax influences ATL development is incompletely understood. A significant fraction of ATL cells contain deletions in HTLV-1 proviral DNAs. In these cells, *tax* coding sequence is preferentially retained, implicating its role in ATL development (Korber *et al*, 1991). ATL cells in general do not express HTLV-1

*Corresponding author. Department of Microbiology and Immunology, Uniformed Services University of the Health Sciences, 4301 Jones Bridge Road, Bethesda, MD 20814, USA. Tel.: +1 301 295 9624; Fax: +1 301 295 1545; E-mail: giam@bob.usuhs.mil

Received: 7 July 2005; accepted: 27 February 2006

sequence, suggesting that *tax* likely affects the early stage of the disease and persistent *tax* expression is not needed for maintenance of the neoplasm (Franchini *et al*, 1984). This distinguishes *tax* from viral oncogenes such as the human papilloma virus E6 and E7 whose constitutive expression is needed for cell transformation.

Tax activates viral transcription by interacting with CREB/ATF-1 and by recruiting transcriptional co-activators, CBP/p300, to three CRE-containing 21-bp repeat enhancer elements in the viral long terminal repeat. The activation of NF- κ B by Tax is a result of the constitutive activation of I- κ B kinase (IKK) by Tax, due in part to a direct interaction between Tax and the γ -subunit of IKK, IKK γ (Chu *et al*, 1998; Yamaoka *et al*, 1998; Jin *et al*, 1999; Sun and Ballard, 1999; Xiao and Sun, 2000). Recent data indicate that via a tripartite interaction, Tax, protein phosphatase 2A (PP2A), and IKK γ form a stable ternary complex, wherein PP2A activity is inhibited or diminished by Tax (Fu *et al*, 2003), thereby maintaining IKK in a phosphorylated and active state.

Tax perturbs critical steps in cell cycle progression (see Jeang *et al* (2004) for a review). Some of these effects of Tax are thought to lead to cell transformation. We have recently observed that Tax causes a reduction in the levels of cyclin B1 and securin prior to mitosis (Liu *et al*, 2003). This activity of Tax is seen in both *Saccharomyces cerevisiae* and HeLa cells. Analyses of *S. cerevisiae* mutants have indicated that the Cdc20-anaphase promoting complex (APC^{Cdc20}) mediates this function of Tax (Liu *et al*, 2003). APC^{Cdc20} is an E3 ubiquitin ligase that becomes active during mitosis, and controls metaphase to anaphase transition by targeting the destruction of cyclin A, securin, and cyclin B1. Recent data indicate that Tax directly binds and activates APC during S phase (Liu *et al*, 2005), causing polyubiquitination and degradation of cyclin A, cyclin B1, and securin before the onset of M phase (Liu *et al*, 2005). The Tax-induced loss of mitotic regulators is associated with delay in cell cycle progression, DNA aneuploidy, and formation of micro-, bi-, and multinucleated cells (Liang *et al*, 2002; Liu *et al*, 2003).

We now show that the cell cycle dysregulation induced by *tax* does not end with mitotic abnormalities. HeLa cells transduced with *tax*, after passage through a faulty cell division cycle, immediately became arrested with G₁ DNA content (termed G₁ arrest or *tax*-induced rapid senescence, *tax*-IRS herein). They expressed high levels of Cdk2 inhibitors: p21^{CIP1/WAF1} and p27^{KIP1} and displayed phenotypes indistinguishable from cells in senescence (Dimri *et al*, 1995). Expression of *tax* during G₁ or early G₁/S does not lead immediately to a cessation of the cell cycle; rather, the senescence caused by Tax depends upon transit through S/G₂/M wherein a dramatic and persistent rise in p21^{CIP1/WAF1} and p27^{KIP1} occurs in mid to late S, G₂/M, leading up to the arrest.

The destruction of p21^{CIP1/WAF1} and p27^{KIP1} occurs during S phase and is regulated by the multisubunit E3 ubiquitin ligase, SCF (Skp-Cullin-F box), in association with its

substrate-targeting subunit, Skp2 (Carrano *et al.*, 1999; Nakayama *et al.*, 2000, 2004; Bornstein *et al.*, 2003; Bashir *et al.*, 2004; Wei *et al.*, 2004) and the cell cycle regulatory protein, Cks1 (Ganoth *et al.*, 2001; Bashir *et al.*, 2004; Wei *et al.*, 2004). We found that in *tax*-expressing cells, Skp2 also became polyubiquitinated and degraded during S phase. The decline in Skp2 appears to cause inhibition of SCF^{SKP2} and stabilization of p21^{CIP1/WAF1} and p27^{KIP1}, thereby committing HeLa cells to rapid senescence. Transcriptional activation of p21^{CIP1/WAF1} by Tax has been previously reported (Akagi *et al.*, 1996; Chowdhury *et al.*, 2003; de la Fuente *et al.*, 2003; Kawata *et al.*, 2003). Despite abundant Tax and p21^{CIP1/WAF1} expression, HTLV-1-transformed T cells grow and proliferate normally. They invariably express low levels of p27^{KIP1} mRNA and protein, in contrast to HeLa cells newly transduced with *tax*. The difference in the p27^{KIP1} status in HTLV-1-transformed cells and *tax*-transduced HeLa cells strongly implicates loss or inactivation of p27^{KIP1} as a critical step in T-cell transformation by Tax and HTLV-1. Indeed, Tax could be stably expressed in p27^{KIP1}-null NIH3T3 cells but not in p21^{CIP1/WAF1}-null cells. We propose that a loss of p27^{KIP1} functions is necessary for *tax*-expressing cells to evade *tax*-IRS. This allows the transforming properties of Tax, including potent activation of IKK-NF- κ B, activation of Cdk4, and induction of chromosome instability to take effect, leading to cell transformation and ATL.

Results

Tax-transduced HeLa cells become permanently G₁-arrested

We have shown recently that Tax directly interacts with APC and activates it in an unscheduled manner, causing the polyubiquitination and degradation of cyclin A, cyclin B1, and securin in *S. cerevisiae*, HeLa, and human T cells before the onset of mitosis (Liu *et al.*, 2003, 2005). The premature APC activation by Tax is accompanied by a delay in S/G₂/M progression, and severe mitotic abnormalities including DNA aneuploidy, cytokinesis failure, and formation of micro-, bi-, and multinucleated cells (Liang *et al.*, 2002; Liu *et al.*, 2003).

To explore the biological effects of *tax* further, we produced a *tax* lentivirus vector, LV-Tax, and a control green fluorescence protein vector, LV-GFP, using the HR'-CMV plasmid (Naldini *et al.*, 1996). A packaging plasmid, pCMV Δ R8.2 Δ vpr, (kindly provided by Dr Irvin Chen) deleted for *env* and *vpr*, together with a VSV-G (vesicular stomatitis virus glycoprotein) expression plasmid were used for vector production. The deletion of *vpr* in pCMV Δ R8.2 Δ vpr eliminated Vpr from vector particles and prevented Vpr-induced G₂/M arrest and apoptosis. LV-Tax and LV-GFP particles were produced as in Materials and methods. Asynchronously growing HeLa cells were then transduced with LV-Tax or LV-GFP at a multiplicity of infection (m.o.i.) of 5. Interestingly, LV-Tax-transduced cell population ceased growing within 3–4 days, and accumulated many binucleated cells (marked with arrows, Figure 1 LV-Tax panel, see also Figure 3B). The LV-Tax cells were enlarged, granulated, and assumed a flattened morphology (Figure 1). By contrast, LV-GFP cells continued to proliferate (note the round and refractive mitotic cells) with typical HeLa morphology (Figure 1 LV-GFP panel).

To characterize further the LV-Tax cells, we examined their progression through successive cell cycles. HeLa cells were

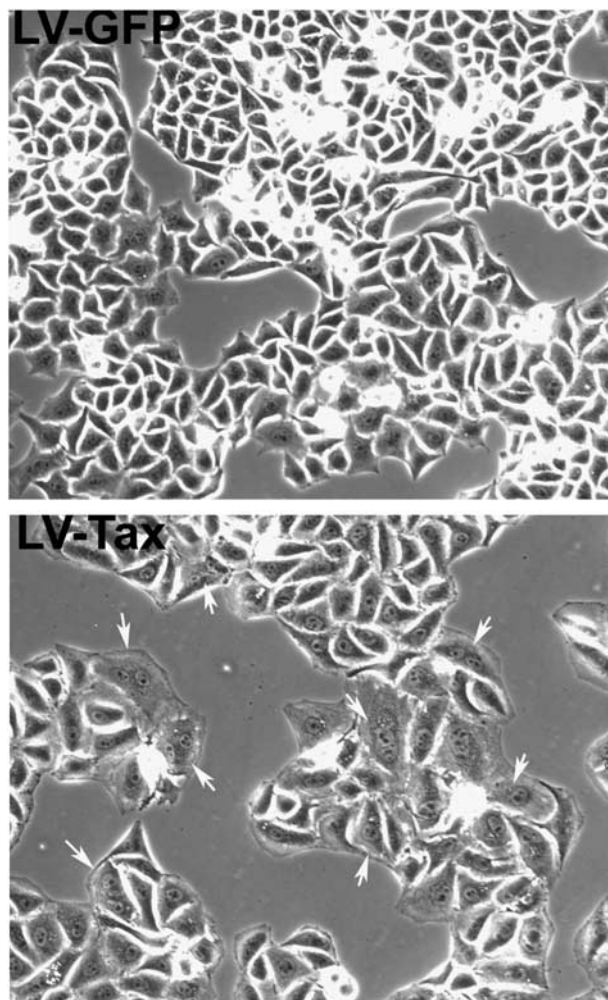


Figure 1 Altered morphology of HeLa cells transduced by LV-Tax. Asynchronously growing HeLa cells were plated at a density of 2.5×10^4 cells/well in six-well plates and transduced with LV-Tax or LV-GFP at an m.o.i. of 5, grown for 3 days, and photographed. Binucleated or micronucleated cells are marked with arrows.

first synchronized at G₁/S border with a double-thymidine block (DTB), released from the arrest for 1 h, and then infected with LV-Tax or LV-GFP. Because reverse transcription, like cellular DNA synthesis, is inhibited by the thymidine block, entry into S is necessary for lentivirus vector-mediated gene transduction. The LV-transduced cells were then collected at the indicated times after release for flow cytometry. The LV-GFP cells maintained synchrony within 62 h after release, and cycled normally (note the undulation of G₁ populations in Figure 2A LV-GFP panel). In striking contrast, and consistent with microscopic observations (Figure 1), most LV-Tax cells reached G₁ at or before 38 h after release and ceased cycling beyond that point (note the lack of undulation of G₁ populations in Figure 2A LV-Tax panel). A portion of the LV-Tax cells (20%) also accumulated with 4N DNA content (Figure 2B, 40 & 56 h). The appearance of this cell population coincided with the emergence of binucleated LV-Tax cells (Figure 1).

As reported previously (Liu *et al.*, 2003), LV-Tax-transduced cells showed a delay in G₂/M progression prior to the G₁ arrest, as evidenced by a considerable G₂/M population at 30 h post-release, a time when most LV-GFP cells had exited

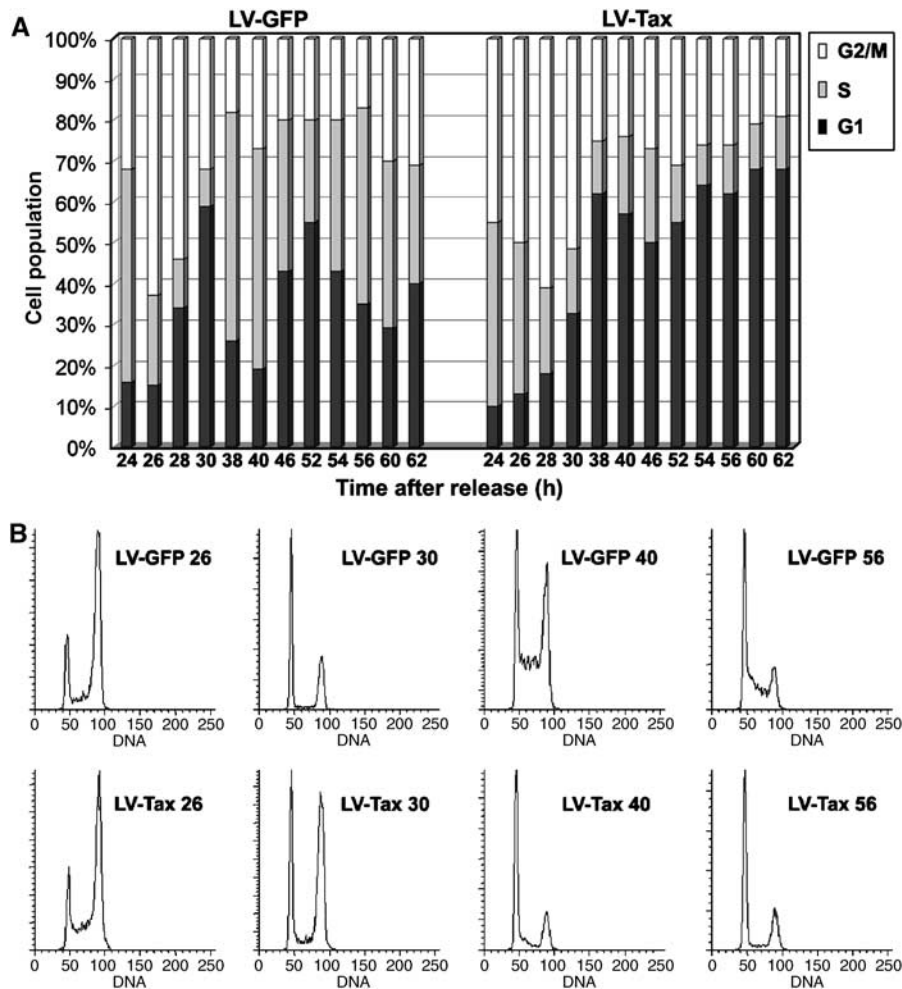


Figure 2 LV-Tax-transduced cells became G₁-arrested after passage through an abnormal cell cycle. **(A)** Comparison of cell cycle progression of LV-GFP- and LV-Tax-transduced HeLa cells by flow cytometry. HeLa cells were first synchronized by DTB, released from the arrest for 1 h, and then infected with LV-Tax or LV-GFP at an m.o.i. of 5. The cells were then collected at the indicated times (24, 26, 28, 30, 38, 40, 46, 52, 54, 56, 60, and 62 h) after release for flow cytometry. The percentages of cells in G₁ (solid), S (gray), and G₂/M (open) phases of the cell cycle at a given time were computed using the ModFit LT software package. **(B)** Flow cytometry histogram of propidium iodide-stained HeLa cells transduced with LV-GFP or LV-Tax vector (samples collected at 26, 30, 40, and 56 h post-release are shown, ordinate: cell numbers; abscissa: DNA content).

mitosis (Figure 2B, compare the G₂ populations at 26 and 30 h after release: LV-GFP 26 versus LV-Tax 26, and LV-GFP 30 versus LV-Tax 30). After the mitotic delay, the bulk of LV-Tax cells were arrested with G₁ DNA content (Figure 2B compare LV-GFP 40 versus LV-Tax 40 and LV-GFP 56 versus LV-Tax 56). Based on the 16-h doubling time of control HeLa cells, we calculated the point of the cell cycle at which LV-Tax cells became arrested (at or prior to 38 h post-release) to be the second G₁ phase after release from DTB. That LV-Tax cells became arrested at the second, but not the first G₁ phase immediately after *tax* transduction is most likely because 12–24 h is needed for reverse transcription, integration, and *tax* expression. Indeed, HeLa cells transduced with Ad-Tax, an adenovirus vector that allows immediate *tax* expression after infection, arrested in the first G₁ phase (Figure 5).

Tax-induced G₁ arrest is indistinguishable from cellular senescence

The phenotypes of *tax*-transduced cells—cessation of cell proliferation, permanent G₁ arrest with enlarged, granulated

and flattened cell shape—resemble cellular senescence seen in aging cells, cells treated with chemotherapeutic chemicals (Chang *et al.*, 1999), primary cells expressing activated form of *ras* (Serrano *et al.*, 1997), and HeLa cells whose p53 and pRB pathways have been activated by a repression of HPV-18 (human papilloma virus type 18) E6 and E7 expression (Wells *et al.*, 2000, 2003). To characterize the LV-Tax cells further, we determined their levels of p16^{INK4a}, p21^{CIP1/WAF1}, and p27^{KIP1}, CDK inhibitors, and stained them for the senescence-associated β-galactosidase (SA-β-Gal) (Dimri *et al.*, 1995). The level of p16^{INK4a} in LV-Tax cells was similar to that of LV-GFP cells 3 days after transduction (Figure 3A). By contrast, the LV-Tax cells expressed prodigious amounts of p21^{CIP1/WAF1} and p27^{KIP1} (Figure 3A), and stained positive for the SA-β-Gal (Figure 3B). The levels of cyclin B1 and securin in LV-Tax cells were low or undetectable, consistent with their degradation induced by Tax and/or the cessation of cell proliferation. As anticipated, LV-GFP cells showed no sign of senescence (Figure 3B). The growth-arrested LV-Tax cells persisted in culture and remained metabolically active for at least 2 weeks (not shown). These results strongly suggest that immediately

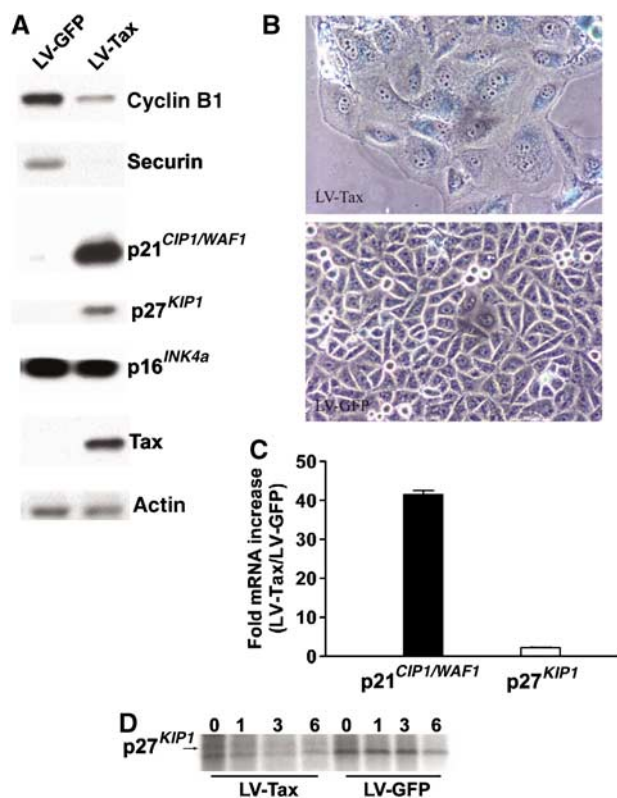


Figure 3 G₁-arrested *tax*-expressing cells are in senescence. (A) Immunoblots of HeLa cells transduced with LV-Tax or LV-GFP. Cell lysates were prepared and immunoblotted using cyclin B1, human securin (Securin), p21^{CIP1/WAF1}, p27^{KIP1}, p16^{INK4a}, Tax, and actin antibodies as described. (B) Expression of the senescence-associated β-galactosidase (SA-β-Gal) in HeLa cells transduced with LV-Tax. Asynchronously growing HeLa cells (2.5 × 10⁴ cells/well in six-well plates) were transduced with LV-Tax or LV-GFP at an m.o.i. of 5, grown for 3 days, and stained with X-Gal overnight at 37°C (see Materials and methods). (C) Ratios of p21^{CIP1/WAF1} and p27^{KIP1} mRNA levels in LV-Tax- versus LV-GFP-transduced cells. Quantitative real-time RT-PCR was as in Materials and methods. Four RT-PCRs were carried out for each RNA species (p21^{CIP1/WAF1}, p27^{KIP1}, and β-actin) in LV-Tax and LV-GFP cells. The relative mRNA levels of p21^{CIP1/WAF1} and p27^{KIP1} were quantified by normalizing against that of β-actin. The fold increases of p21^{CIP1/WAF1} and p27^{KIP1} mRNAs (LV-Tax/LV-GFP) were then calculated and plotted. (D) Pulse chase of p27^{KIP1} in LV-Tax- versus LV-GFP-transduced HeLa cells. Pulse chase and immunoprecipitation were carried out as in Materials and methods. The times after chase (0, 1, 3, 6 h) are indicated.

after an aberrant cell cycle, *tax*-transduced cells entered into senescence.

Tax has been reported to activate p21^{CIP1/WAF1} expression previously (Akagi *et al.*, 1996; Chowdhury *et al.*, 2003; de la Fuente *et al.*, 2003; Kawata *et al.*, 2003); however, transcriptional activation of p27^{KIP1} by Tax has not been observed (Cereseto *et al.*, 1999). To confirm these data, we performed quantitative real-time RT-PCR on total RNA samples prepared from LV-GFP and LV-Tax cells 3 days after infection. Indeed, the mRNA level of p21^{CIP1/WAF1} in LV-Tax-transduced HeLa cells was 40-fold of that in LV-GFP-transduced control, while the level of p27^{KIP1} mRNA in LV-Tax cells was only two-fold than that of the control (Figure 3C). We infer that the great surge in p21^{CIP1/WAF1} level is due, in part, to activation of mRNA transcription by Tax, but the increase in p27^{KIP1} in LV-Tax cells cannot be accounted for by transcriptional

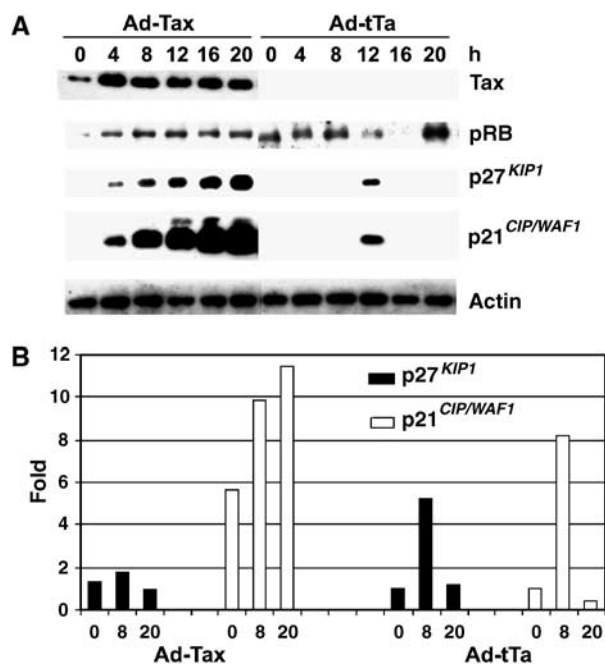


Figure 4 Tax-induced surge in p21^{CIP1/WAF1} and p27^{KIP1} occurs independently of p53 and pRB. (A) Immunoblots of HeLa cells infected with Ad-Tax or Ad-tTa. HeLa cells were synchronized as described for Figure 1. At the start of the second thymidine treatment, cells were infected with either Ad-Tax or Ad-tTa (negative control) at an m.o.i. of 5. After release, cells were collected at 0, 4, 8, 12, 16, and 20 h, and immunoblotted using Tax, p27^{KIP1}, p21^{CIP1/WAF1}, pRB, and β-actin antibodies. (B) Relative p27^{KIP1} and p21^{CIP1/WAF1} mRNA levels in Ad-Tax- versus Ad-tTa-transduced HeLa cells. Total cellular RNAs from samples at 0, 8, and 20 h post-release were prepared as in Materials and methods. RT-PCR was carried out as in Figure 3 and normalized against the p27^{KIP1} or p21^{CIP1/WAF1} mRNA level of Ad-tTa-transduced cells at 0 h post-release.

activation alone. A pulse-chase experiment showed that the half-life of p27^{KIP1} in HeLa cells became greatly increased in the presence of Tax (Figure 3D). As indicated, p27^{KIP1} was barely detectable 1 h after chase in LV-GFP cells, but persisted at 6 h after chase in LV-Tax cells. Therefore, stabilization of p27^{KIP1}, and possibly p21^{CIP1/WAF1}, plays a critical role in their build-up in *tax*-transduced cells.

Tax-induced rapid, senescence (*tax*-IRS) occurs independently of p53 and pRB

Cellular senescence induced by the oncogenic *ras* is p53- and p16^{INK4a}/pRB-mediated (Wells *et al.*, 2000, 2003). The *tax*-mediated G₁ arrest/senescence observed here occurred in HPV-18-transformed HeLa cells whose p53 is targeted for degradation by the HPV-18 E6 (Scheffner *et al.*, 1990), and whose pRB is inactivated by HPV-18 E7 (reviewed in Helt and Galloway, 2003). This suggests that *tax*-induced rapid senescence (*tax*-IRS) occurs in a p53- and pRB-independent manner. To rule out the possibility that Tax indirectly stabilized p53 or pRB in HeLa cells, we examined their protein levels throughout cell cycle progression. HeLa cells were again arrested at G₁/S with DTB. At the start of the second thymidine treatment, cells were infected with Ad-Tax or control Ad-tTa (an adenovirus vector for *tax* or a control vector for tet-transactivator) for 16 h, released from the arrest, and blotted for p53, pRB, p21^{CIP1/WAF1}, and p27^{KIP1}. Despite a sharp rise in p21^{CIP1/WAF1} and p27^{KIP1} in Ad-Tax cells

(Figure 4), the levels of p53 in Ad-tTa- and Ad-Tax HeLa cells were low or undetectable throughout the cell cycle progression (not shown). The level of pRB in control Ad-tTa cells rose slightly during G₂/M/G₁ and fell during S. By contrast, pRB cycling was not observed in Ad-Tax cells, possibly due to the cessation of cell cycle activities caused by Tax. Importantly, the level of pRB in Ad-Tax-infected cells remained comparable to that in the Ad-tTa control (Figure 4). Finally, consistent with the data in Figure 3C, Tax greatly induced p21^{CIP1/WAF1} mRNA transcription but had only a minor effect on p27^{KIP1} mRNA levels (Figures 3C and 4B). The Tax-mediated increase in p27^{KIP1} is therefore exerted at the level of protein stabilization as indicated in Figure 3D. These results indicate that the rapid cellular senescence induced by Tax occurs in a p53- and pRB-independent manner, apparently via a mechanism distinct from that executed by oncogenic *ras*, and involves transactivation of p21^{CIP1/WAF1} and stabilization of both p21^{CIP1/WAF1} and p27^{KIP1}. As expected, *tax* also induced rapid senescence in p53-null human SKOV ovarian cancer cells and proliferative arrest in *S. cerevisiae* (not shown).

Premature APC activation by Tax is accompanied by p21^{CIP1/WAF1} and p27^{KIP1} increase

Temporally, the rise in p21^{CIP1/WAF1} and p27^{KIP1} *tax*-expressing cells occurred in S/G₂ phase (Figure 4). It paralleled premature APC activation by Tax (Liu *et al.*, 2003, 2005). This prompted us to examine the connection between premature APC activation and the increase of p21^{CIP1/WAF1} and p27^{KIP1}. To this end, HeLa cells were again arrested and infected with Ad-Tax and Ad-tTa as above, released from the arrest, and analyzed. As reported (Liu *et al.*, 2003) and indicated by flow cytometry, expression of *tax* during the G₁/S block did not result in cell cycle arrest immediately (Figure 5A). Rather, Ad-Tax cells transited through S/G₂/M with a 4–5 h delay (compare Ad-Tax and Ad-tTa at 12 h post-release) and then came to a complete stop at the next G₁ (Figure 5A top panel, Ad-Tax, 16–28 h post-release). By contrast, Ad-tTa cells progressed normally through S and G₂/M after release, and readily initiated another cell cycle (Figure 5A bottom panels, 16–20 h post-release). In control Ad-tTa cells, the levels of p21^{CIP1/WAF1} and p27^{KIP1} are cyclical—increased moderately during G₁ (Figure 5B, Ad-tTa, 12 h post-release, see Figure 4 also), and became undetectable during S/G₂/M (Figure 5B, 0–8 h post-release, and 16 and 20 h post-release). As expected, levels of cyclin A and B1, and securin in Ad-tTa cells cycled normally—rose sharply during S and declined abruptly after mitosis (Figure 5B right panels, compare 8 and 12 h post-release). In sharp contrast and as previously reported, the levels of cyclins A and B1, and securin in Ad-Tax cells increased but with a significant delay (Figure 5B left panels, compare 8 and 12 h post-release), and never achieved the levels seen in Ad-tTa cells. The reduction in cyclin A, cyclin B1, and securin during the S phase (0–7 h post-release) was concurrent with or was followed immediately by a rise in levels of p21^{CIP1/WAF1} and p27^{KIP1} (8–20 h post-release) during mid to late S, through G₂/M and up to the subsequent G₁ (Figure 5, also see Figure 4). Most likely as a result of the great surge in p21^{CIP1/WAF1} and p27^{KIP1}, cell cycle progression, and cell proliferation ceased abruptly (see Figure 5A top four panels on the right and Figure 5B, Ad-Tax 12–20 h post-release). These temporal correlations raise the possibility

that the unscheduled APC activation by Tax and the increase in p21^{CIP1/WAF1} and p27^{KIP1} may be causally linked or may have the same cause.

Unscheduled activation of APC by Tax correlates with a loss of Skp2 and a surge in the levels of p21^{CIP1/WAF1} and p27^{KIP1}

The levels of p21^{CIP1/WAF1} and p27^{KIP1} are regulated through phosphorylation (by cyclinE/Cdk2), ubiquitination, and proteasome-mediated degradation (Swanson *et al.*, 2000; Hara *et al.*, 2001; Bornstein *et al.*, 2003). The E3 ubiquitin ligase, SCF, together with its substrate-recognition subunit, Skp2, is responsible for the ubiquitination and degradation of p21^{CIP1/WAF1} and p27^{KIP1} (Ganoth *et al.*, 2001; Bashir *et al.*, 2004; Wei *et al.*, 2004). Degradation of p27^{KIP1} also requires its presentation by the cyclin A-Cdk2 complex to SCF^{Skp2} (Zhu *et al.*, 2004). The level of Skp2 oscillates in a cell cycle-dependent manner (see Figure 5B, Ad-tTa set, compare 8 and 12 or 16 h after release). Two recent reports (Bashir *et al.*, 2004; Wei *et al.*, 2004) showed that Skp2 and another SCF subunit, Cks1, are substrates of the Cdh1-associated APC (APC^{Cdh1}). Both become ubiquitinated and degraded in late M and early G₁ when APC^{Cdh1} is highly active. This renders SCF inactive and allows p21^{CIP1/WAF1} and p27^{KIP1} to accumulate transiently in G₁ (also see Figure 5B Ad-tTa, 12 h post-release). The links between APC^{Cdh1}, SCF^{Skp2}, and the levels of p21^{CIP1/WAF1} and p27^{KIP1}, together with the data showing that Tax activates APC ahead of schedule (Liu *et al.*, 2003, 2005) led us to examine the status of Skp2 in response to Tax. Consistent with the results previously reported (Bashir *et al.*, 2004; Wei *et al.*, 2004), in the Ad-tTa control, Skp2 accumulated during S phase and became degraded during G₁, which was accompanied by a moderate and transient accumulation of p21^{CIP1/WAF1} and p27^{KIP1} (Figure 5B, Ad-tTa, 12 h post-release). By contrast, in parallel with the decrease in cyclin A, cyclin B1, and securin, the level of Skp2 was also reduced in Ad-Tax cells (Figure 5B, Ad-Tax, 4–12 h post-release). The Skp2 mRNA levels in Ad-Tax cells were approximately 80% of the Ad-tTa controls as quantitated by RT-PCR (not shown), indicating that the Tax-induced decrease in Skp2 protein is not due to transcriptional repression. Importantly, the highest level of Skp2 under *tax*-positive condition (Figure 5B, Ad-Tax, S phase, 0–7 h post-release) is comparable to the lowest levels of Skp2 under *tax*-negative condition (Figure 5B, Ad-tTa, G₁, 12 and 16 h post-release). Finally, Skp2 declined further when the Ad-Tax cells eventually exited mitosis and entered into permanent G₁ arrest (Figure 5B, Ad-Tax, G₁, 20 h post-release and Figure 5A 20, 24, and 28 h post-release). These results strongly suggest that the loss of Skp2 and inactivation of SCF^{Skp2} occur as a consequence of APC activation by Tax. This in turn causes stabilization of p21^{CIP1/WAF1} and p27^{KIP1}, committing cells to irreversible G₁ arrest/senescence.

Tax activates polyubiquitination of Skp2 during S phase

To demonstrate that Tax directly cause polyubiquitination and degradation of Skp2, asynchronously growing HeLa cells were transfected with HA-tagged ubiquitin, CMV-HA-Ub, together with CMV-Flag-Skp2. On the second day, transfected cells were infected with Ad-Tax or Ad-tTa for 16 h and treated with the proteasome inhibitor, MG132, for 4 h. Cell

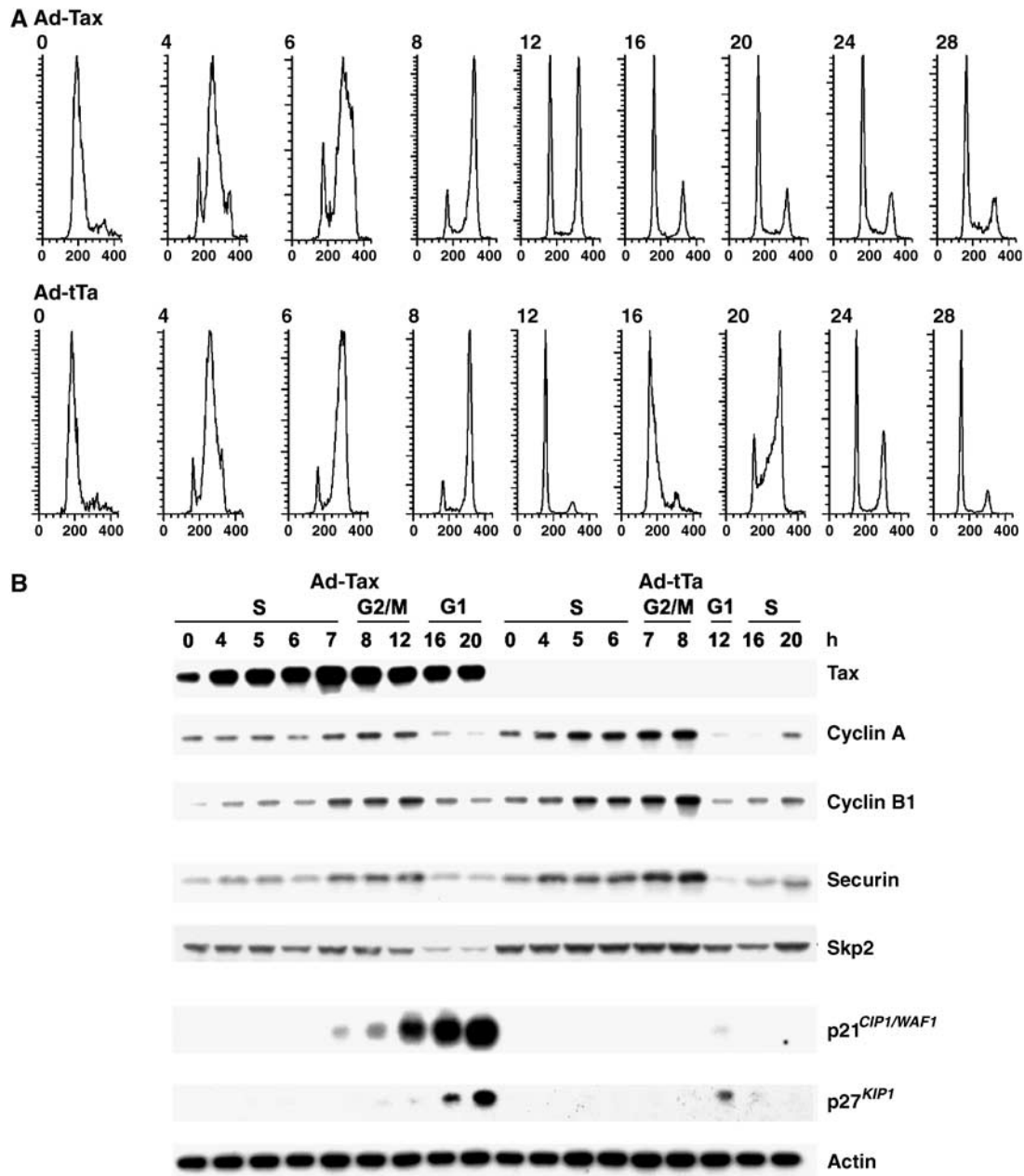


Figure 5 Unscheduled activation of the APC by Tax leads to a loss of Skp2 and stabilization of p21^{CIP1/WAF1} and p27^{KIP1}. HeLa cells were synchronized and infected with Ad-Tax or Ad-tTa as in Figure 4. Cells were then collected at the indicated times after release for flow cytometry (0, 4, 6, 8, 12, 16, 20, 24, and 28 h) and immunoblotting (0, 4, 5, 6, 7, 8, 12, 16, and 20 h). (A) Flow cytometry of propidium iodide-stained HeLa cells transduced with Ad-Tax and Ad-tTa, respectively. Inclusion of later time points (24 and 28 h post-release) is made to highlight the G₁ arrest of *tax*-expressing cells. For each panel, the ordinate represents cell numbers; the abscissa, DNA content. (B) Immunoblots of cyclin A, cyclin B1, securin, Skp2, p21^{CIP1/WAF1}, p27^{KIP1}, and actin. Cell lysates from Ad-Tax (left panels)- or Ad-tTa (right panels)-transduced cells were collected at the indicated times and immunoblotted. The stage of the cell cycle for each chosen post-release time point was determined based on the flow cytometry results in (A) and indicated at the top of the immunoblots.

lysates were then immunoprecipitated for Skp2 using the Flag-epitope antibody and immunoblotted with the HA antibody to detect the polyubiquitinated Skp2. Consistent with the idea that unscheduled activation of APC by Tax leads to Skp2 degradation, an increase in the level of polyubiquitinated Skp2 was detected in Ad-Tax cells (Figure 6B, left lane) versus Ad-tTa cells (Figure 6B, right lane). We next transfected HeLa cells with both CMV-HA-Ub and CMV-Flag-Skp2, and then synchronized them at G₁/S border. During the

second thymidine block, cells were infected with Ad-Tax or Ad-tTa, and then released into thymidine-free medium containing MG-132. Cell lysates were prepared at multiple time points after the release, immunoprecipitated with the Flag antibody, and immunoblotted with the HA antibody for polyubiquitinated Skp2. As shown in Figure 6A, at 4, 6, and 8 h after release when most cells were transiting through S phase, polyubiquitinated Skp2 was readily detected in the Ad-Tax cells (Ad-Tax, '+' lanes). This contrasts with the

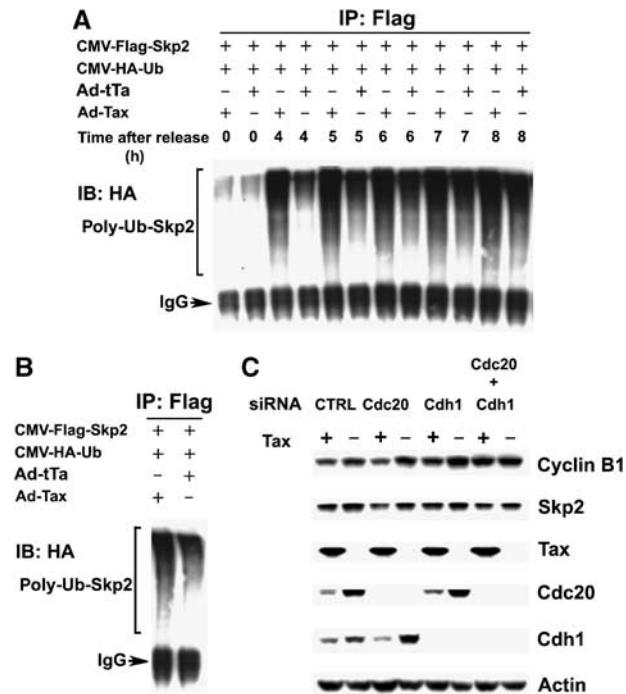


Figure 6 Tax induces polyubiquitination of Skp2 during S phase. (A) Plasmids encoding the HA-tagged ubiquitin (CMV-HA-Ub) and Flag-tagged Skp2 (CMV-Flag-Skp2) were transfected into HeLa cells using the FuGENE 6 Transfection Reagent. The transfected cells were then synchronized with DTB. At the start of the second thymidine treatment, cells were also infected (at an m.o.i. of 5) with Ad-Tax or Ad-tTa as in Figure 4. The cells were then released (for 0, 4, 5, 6, 7, and 8 h) in complete DMEM containing 10 μ M MG132. Immunoprecipitation (IP) of Flag-Skp2 was carried out for lysates collected at each time point (0, 4, 5, 6, 7, and 8 h) after release using the Flag epitope antibody, immunoprecipitates were resolved in an SDS/4–12% PAGE, and immunoblotted (IB) for the polyubiquitinated Skp2 (bracketed) using the HA antibody. (B) Experiments were similar as in (A) except that cells were not synchronized and were infected by Ad-Tax or Ad-tTa for 16 h, then transferred to DMEM containing 10 μ M MG132 for 4 h. (C) APC activation by Tax is inhibited by siRNAs against Cdc20 and Cdh1. siRNA transfection was performed as in Materials and methods. Cells were harvest for immunoblots for cyclin B1, Skp2, Tax, Cdc20, Cdh1, and actin at 8 h post-release from the G₁/S arrest. The siRNA species used are as indicated. Ad-Tax- and Ad-tTa-transduced cells are labeled as Tax + and –, respectively.

Ad-tTa control, wherein polyubiquitinated Skp2 became apparent only at 8 h post-release when cells started to transit mitosis (Ad-tTa, ‘–’ lanes).

Previous results have shown that Tax binds to both APC^{Cdc20} and APC^{Cdh1} (Liu *et al*, 2005). Further, APC^{Cdc20} appears to be sufficient for Tax-induced Clb2 degradation in *S. cerevisiae* (Liu *et al*, 2003). To determine if Tax targets APC^{Cdc20} or APC^{Cdh1} in HeLa cells, siRNA knockdown experiments were performed. HeLa cells were synchronized by DTB, and transfected with a control siRNA, a Cdc20 siRNA, a Cdh1 siRNA, or a combination of both Cdc20 and Cdh1 siRNAs 2 h before the second thymidine block, followed by infection with Ad-Tax or Ad-tTA. As shown in Figure 6C, the delay in cell cycle progression caused by Tax was reflected by a slower rise in levels of Cdc20 and Cdh1 after release from G₁/S arrest. This notwithstanding, siRNA’s directed against Cdc20 and Cdh1 were effective in reducing their expression respectively. Importantly, Tax-induced cyclin B reduction was inhibited partially by siRNA against Cdc20, and to a greater

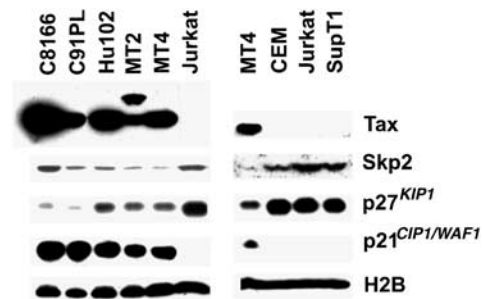


Figure 7 HTLV-I-transformed T cells express high levels of p21^{CIP1/WAF1} but low levels of p27^{KIP1}. (A) Tax, Skp2, p21^{CIP1/WAF1}, p27^{KIP1}, histone 2B (H2B) immunoblots of HTLV-transformed T-cell lines: C8166, C91PL, Hut102, MT2, and MT4 versus HTLV-I-unrelated Jurkat T, CEM, and SupT1 cell lines. (B) Table I. Ratios of Skp2, p21^{CIP1/WAF1}, and p27^{KIP1} mRNAs in HTLV-I-transformed cells, and in CEM and SupT1 cells versus Jurkat T cells. The mRNA ratios were determined as described in Materials and methods.

extent, by siRNA against Cdh1. The greatest inhibition was achieved when both Cdc20 and Cdh1 siRNA’s were used, suggesting that both APC^{Cdc20} and APC^{Cdh1} were affected by Tax (Figure 6C). Finally, in agreement with the role of APC^{Cdh1} in Skp2 degradation, siRNA knockdown of Cdh1 efficiently blocked the loss of Skp2 induced by Tax (Figure 6C).

HTLV-1 transformed T cells express greatly elevated levels of p21^{CIP1/WAF1} but low levels of p27^{KIP1}

The rapid senescence of HeLa cells induced by Tax raises the question how HTLV-1-transformed T-cell lines manage to express *tax* abundantly without undergoing cell cycle arrest. We have shown recently that Tax prematurely activates APC in MT4, C8166, and C91PL cells (Liu *et al*, 2005). The APC activation and reduction of cyclin A, securin, and cyclin B1 in these cells were associated with a delay in S/G₂/M progression, but did not lead to G₁ arrest (Liu *et al*, 2005). Transactivation of p21^{CIP1/WAF1} and premature activation of APC by Tax are expected to increase both p21^{CIP1/WAF1} and p27^{KIP1} protein levels in HTLV-1-transformed T cells. Indeed, five HTLV-1-transformed T-cell lines examined all expressed abundant p21^{CIP1/WAF1} mRNA (20–100 fold) and protein when compared to three HTLV-1-unrelated T-cell lines, Jurkat, CEM, and SupT1 (Figure 7 and Table I). Skp2 mRNA in all transformed lines was approximately 20% that of Jurkat. This is likely a result of the overexpression of Skp2 in Jurkat as previously reported (Lim *et al*, 2002). Compared to Jurkat, CEM cells expressed elevated mRNA levels of both Skp2 and p27^{KIP1} (Table I), while the levels of Skp2, p21^{CIP1/WAF1}, and p27^{KIP1} in control SupT1 were similar to that of Jurkat. As expected, increased polyubiquitination of Skp2 in S phase was readily detected in C8166 cells (not shown). Most interestingly, in contrast to HeLa cells transduced with LV-Tax or Ad-Tax (see Figure 3 for comparison) and in spite of lower Skp2 levels (expected to lead to p27^{KIP1} stabilization), all HTLV-I-transformed cells expressed low to undetectable levels of p27^{KIP1} protein and significantly lower levels of p27^{KIP1} mRNA (13–53%) compared to HTLV-1-unrelated controls (Figure 7 and Table I). Based on these results, we speculate that *tax*-IRS may be principally mediated by p27^{KIP1} and all five independently isolated HTLV-1-transformed T-cell lines examined here have evaded *tax*-IRS through a loss of p27^{KIP1} expression and/or functions (Figure 9).

Table 1 mRNA ratios (HTLV-1-transformed versus HTLV-1-unrelated T-cell lines)

| | p27 ^{KIP1} | p21 ^{CIP1/WAF1} | Skp2 |
|--------|---------------------|--------------------------|-------------|
| C8166 | 0.13 ± 0.02 | 55 ± 5 | 0.20 ± 0.04 |
| C91PL | 0.13 ± 0.03 | 104 ± 16 | 0.17 ± 0.02 |
| HuT102 | 0.53 ± 0.08 | 74 ± 4 | 0.23 ± 0.07 |
| MT2 | 0.41 ± 0.04 | 32 ± 11 | 0.21 ± 0.02 |
| MT4 | 0.55 ± 0.03 | 20 ± 3 | 0.24 ± 0.00 |
| Jurkat | 1 | 1 | 1 |
| SupT1 | 1.5 ± 0.52 | 2.6 ± 1.0 | 1.1 ± 0.40 |
| CEM | 4.1 ± 1.1 | 0.78 ± 0.15 | 4.9 ± 1.2 |

Tax can be stably expressed in p27^{KIP1}-null NIH3T3 cells

To determine if a loss of p27^{KIP1} can prevent tax-IRS, a lentivirus vector containing the *tax* gene and the SV40 promoter-driven puromycin-resistance gene was used to transduce, respectively, a wild-type NIH3T3 cell line, an NIH3T3 cell line with a homozygous deletion of p21^{CIP1/WAF1} gene (p21^{CIP1/WAF1}^{-/-}), and importantly, a NIH3T3 cell line with a homozygous deletion of p27^{KIP1} gene (p27^{KIP1}^{-/-}). While no cell lines that stably express tax could be established in wild-type or p21^{CIP1/WAF1}^{-/-} NIH3T3 background (unpublished results), several *tax*-expressing p27^{KIP1}^{-/-} (*tax* + /p27^{KIP1}^{-/-}) cell clones were readily obtained (Figure 8). These clones have grown continuously for more than 6 months with stable *tax* expression. Interestingly, the doubling time of *tax* + /p27^{KIP1}^{-/-} cells became lengthened compared to that of the parental p27^{KIP1}^{-/-} cells, consistent with the cell cycle slow-down of HTLV-1-transformed T cells previously reported (Liu *et al*, 2005). Finally, flow cytometry of asynchronously growing p27^{KIP1}^{-/-} and *tax* + /p27^{KIP1}^{-/-} (clone 2) cells indicated that Tax significantly reduced S (from 53 to 32%) and increased G₁ and G₂/M cell populations (33–45% and 13–23%, respectively, Figure 8) likely as a result of the premature activation of APC and the transactivation and stabilization of p21^{CIP1/WAF1}^{-/-} (Figure 8). In aggregate, these data support the notion that loss of p27^{KIP1} functions circumvents the G₁ arrest/senescence induced by Tax and is necessary for stable *tax* expression and cell transformation.

Discussion

Tax-IRS is caused by a p53- and pRB-independent mechanism

The cellular mechanisms that trigger the senescence pathway are not fully resolved at present. Prevailing evidence indicates that tumor suppressors such as pRb, p53, and members of the INK and CIP/KIP families of CDK inhibitors play significant roles in this process (Chin *et al*, 1999; Wells *et al*, 2000, 2003; Ferbeyre *et al*, 2002). Present data suggest that the permanent proliferative arrest brought about by *tax* differs mechanistically from that caused by oncogenic *ras*. Unlike oncogenic *ras*, *tax* readily commits immortalized and transformed cells such as HeLa to senescence, and apparently does so without functional p53 and pRB. The *tax*-IRS is accompanied by overt mitotic aberrations, and occurs rapidly after one cell division cycle upon *tax* expression. Whether oncogenic *ras*-induced senescence occurs within or immediately after a single cell division

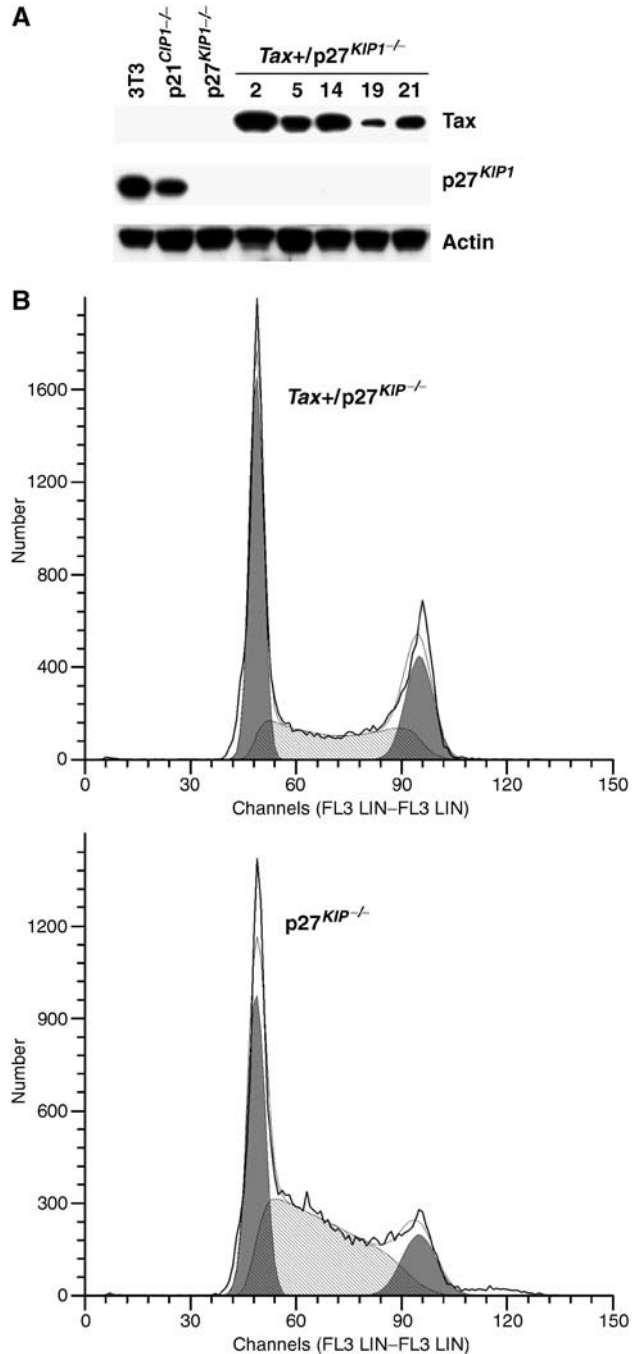


Figure 8 HTLV-I Tax can be stably expressed in p27^{KIP1}-null NIH3T3 cells. (A) A lentivirus vector LV-Tax-Puro, containing *tax* and the SV40 promoter-driven puromycin-resistance gene, was used to transduce a wild-type NIH3T3 cell line, an NIH3T3 cell line with a homozygous deletion of p21^{CIP1/WAF1} gene (p21^{CIP1/WAF1}^{-/-}), and a similar cell line with a homozygous deletion of p27^{KIP1} gene (p27^{KIP1}^{-/-}). No *tax*-expressing stable cell lines were obtained in NIH3T3 or p21^{CIP1/WAF1}^{-/-} background. Tax and p27^{KIP1} immunoblots for five independently isolated puromycin-resistant clones in p27^{KIP1}^{-/-} background are shown. (B) Flow cytometric analyses (G₁ (left peak, dark shade), S (light shade), G₂/M: (right peak, dark shade)) of asynchronously growing parental p27^{KIP1}^{-/-} cells (G₁: 33%, S: 53%, G₂/M: 13%) and cells of *tax* + /p27^{KIP1}^{-/-} clone #2 (G₁: 45%, S: 32%, G₂/M: 23%).

cycle has not been described. Finally, mitotic abnormalities have not been reported to accompany *ras*-mediated senescence.

Activation of APC by Tax ahead of schedule is responsible for the stabilization of p21^{CIP1/WAF1} and p27^{KIP1}

The great increase of p21^{CIP1/WAF1} and p27^{KIP1} in *tax*-transduced cells is likely to be the cause for *tax*-IRS. Both quantitative real-time RT-PCR and pulse-chase experiments have demonstrated that in *tax*-expressing cells, protein stabilization is the primary cause for p27^{KIP1} increase; while both transactivation and protein stabilization are responsible for p21^{CIP1/WAF1} increase. The persistent rise of p21^{CIP1/WAF1} and p27^{KIP1} through S/G₂/M in *tax*-transduced cells also supports the notion that p21^{CIP1/WAF1} and p27^{KIP1} are stabilized.

The stabilization of p21^{CIP1/WAF1} and p27^{KIP1} caused by Tax can be best explained by the premature APC activation during S phase, which sets in motion the early inactivation of SCF^{Skp2}. In support of this notion, the polyubiquitination and loss of Skp2 in *tax*-transduced cells parallels the unscheduled degradation of cyclin A, cyclin B1, and securin temporally, and precedes or is concurrent with the surge of p21^{CIP1/WAF1} and p27^{KIP1} (Figure 6). Skp2 is a natural substrate of APC^{Cdh1} during late M/early G₁ (Bashir *et al*, 2004; Wei *et al*, 2004). Present data support the idea that the target of Tax activation is APC rather than Cdc20 or Cdh1. In Tax-expressing HeLa cells, both APC^{Cdh1} and APC^{Cdc20} contribute to the reduction in cyclin B1 level (Figure 6C). The most dramatic reduction in Skp2 and increase in p21^{CIP1/WAF1} and p27^{KIP1} occurred when Tax+ cells entered G₁. This is consistent with the notion that at the late stage of mitotic progression, Tax-activated APC^{Cdh1} plays a major role in stabilizing p21^{CIP1/WAF1} and p27^{KIP1}. Indeed, siRNA knock-down of Cdh1 effectively dampened the loss of Skp2 induced by Tax (Figure 6C). Previous analyses of *S. cerevisiae* mutants have suggested that Cdh1 is not required for Tax-induced loss of Clb2 and cell cycle arrest (Liu *et al*, 2003). It is not clear whether this is due to a difference in the manner by which Cdh1 is regulated in *S. cerevisiae* versus HeLa cells, or alternatively, *S. cerevisiae* APC^{Cdc20} may contribute to Tax-induced Skp2 degradation. In conclusion, the loss of cyclin A, cyclin B1, and securin as caused by Tax leads to mitotic aberrations/chromosomal instability (Figures 1 and 3); while the loss of Skp2 and the rise in p21^{CIP1/WAF1} and p27^{KIP1} independently commits cells to *tax*-IRS (Figures 2, 3 and 8). These results are summarized in a model depicted in Figure 9.

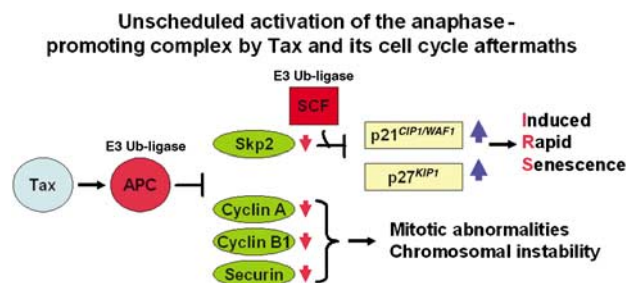


Figure 9 Unscheduled activation of the APC by HTLV-1 Tax and its cell cycle aftermaths. Unscheduled activation of the APC during S phase by HTLV-1 Tax leads to degradation of cyclin A, cyclin B1, and securin, causing mitotic abnormalities/chromosome instability. Concurrently, the degradation of Skp2 results in inhibition/inactivation of SCF^{Skp2}, which, in concert with the loss of cyclin A, leads to the stabilization of p21^{CIP1/WAF1} and especially p27^{KIP1}, committing cells to rapid senescence.

APC activation by Tax requires cellular transit through S phase. During the G₁/S arrest, no accumulation of p21^{CIP1/WAF1} and p27^{KIP1} occurred in spite of Tax expression (Figures 4 and 5). Only after transit to the mid to late S phase did the *tax*-transduced cells begin to accumulate p21^{CIP1/WAF1} and p27^{KIP1}. We think this is because the cellular factors needed for APC activation, such as the polo-like kinase and Cdc20 are destroyed during mitotic exit and synthesized during S phase. Thus, only when these factors are restored during S phase is Tax able to act.

The downregulation of p27^{KIP1} in S and G₂ is impaired in Skp2^{-/-} cells (Hara *et al*, 2001). This has led to the suggestion that the role of Skp2 may be to control p27^{KIP1} during S and G₂ (Hara *et al*, 2001). That the Tax-induced loss of Skp2 and rise of p21^{CIP1/WAF1} and p27^{KIP1} occur during S and G₂ is consistent with this conclusion. The loss of Skp2 alone, however, cannot be the sole cause for the build-up of p21^{CIP1/WAF1} and p27^{KIP1} and *tax*-IRS. Skp2^{-/-} mice are viable. Although Skp2^{-/-} cells accumulate p27^{KIP1}, they do not become G₁ arrested and commit senescence (Nakayama *et al*, 2004). If a loss of Skp2 cannot account fully for the *tax*-IRS, then what can? Koff and co-workers have shown recently that the degradation of p27^{KIP1} requires noncatalytic involvement of cyclin A-Cdk2 (Zhu *et al*, 2004). Therefore, the premature loss of cyclin A induced by Tax likely also contributes to p27^{KIP1} stabilization. Cks1, another subunit of SCF^{Skp2}, is also a target of APC^{Cdh1} (Ganoth *et al*, 2001; Bashir *et al*, 2004; Wei *et al*, 2004). It is possible that Tax also promotes the loss of Cks1 through unscheduled APC activation, thereby add to the severity of SCF^{Skp2} inhibition (Figure 9). Based on these considerations, we speculate that unscheduled activation of APC in S phase (by Tax or other compounds) may be exploited as a means to arrest the proliferation of cancer cells whose p53 and pRB pathways are no longer functional.

Tax-IRS and the development of ATL

HTLV-1 causes ATL in a small percentage (2–6%) of infected individuals after a long latency period of up to 20–40 years. How HTLV-1 infection progresses from clinical latency to full-blown T-cell malignancy is not well understood. The long incubation period and the low frequency of clinical progression to ATL suggest that complex and interdependent viral and cellular events are involved. ATL patients show evidence of a monoclonal integration of HTLV-1 proviral DNA in CD4⁺CD25⁺ leukemia cells. Leukemia/lymphoma apparently emerges from a pool of HTLV-1-positive CD4⁺ T cells that persist for decades in infected individuals, possibly through oligoclonal expansion. How might *tax* affect ATL development? The analyses of HTLV-1-transformed T-cell lines and the stable expression of *tax* in p27^{KIP1}^{-/-} cells (Figure 7) indicate that abrogation and/or inactivation of p27^{KIP1} (complete loss, haplo-insufficiency, transcriptional repression, and/or inactivating phosphorylation of p27^{KIP1}) may allow HTLV-1-infected cells to evade *tax*-IRS and allow the mitogenic activity of *tax* and the chromosomal instability it induces to take effect, leading to cell transformation and development of ATL. Finally, chromosomal instability induced by Tax and host cytotoxic T-lymphocyte response against Tax may then select for a complete loss of *tax* expression from ATL. Examination of HTLV-1-transformed and ATL cells for the status of p27^{KIP1} gene and/or pathways

that inactivate p27^{KIP1} is likely to provide useful clues for the emergence, progression, and treatment of ATL.

Materials and methods

Cell lines

HeLa, 293T, NIH3T3, and NIH3T3 with a homozygous deletion of p21^{CIP1/WAF1} (p21^{CIP1/WAF1}^{-/-}) or p27^{KIP1} gene (p27^{KIP1}^{-/-}) (provided by Dr Andrew Koff, Memorial Sloan-Kettering Cancer center, New York) were grown in Dulbecco's modified Eagle's medium (DMEM). HTLV-transformed T cells, C8166, C91PL, Hut102, MT2, and MT4, and HTLV-unrelated T-cell lines, Jurkat, CEM, and SupT1, were grown in RPMI medium. All media were supplemented with 10% fetal bovine serum (FBS), 2 mM L-glutamine, and 100 U/ml each of penicillin and streptomycin.

Plasmids and antibodies

The lentivirus vector for *tax*, LV-Tax, was derived by inserting a *Bam*HI-*Sal*I fragment containing the coding sequence of the HTLV-1 *tax* into the *Bam*HI and *Xho*I sites of the pHR'CMV-LacZ vector (Naldini *et al.*, 1996) in place of the *lacZ* gene. The control LV-GFP vector was similarly constructed by replacing the *lacZ* gene with the EGFP gene on a *Bam*HI-*Kpn*I fragment. A lentivirus vector, LV-Tax/puromycin, containing *tax* and the puromycin-resistance gene was derived by inserting an *Eco*R1-*Kpn*I fragment containing the SV40 promoter and the puromycin-resistance gene downstream of the Tax cDNA.

The antibody for Tax (4C5) was made in this lab; others include cyclin A (SC-751), cyclin B1 (SC-752), p21^{CIP1/WAF1} (SC-397), p27^{KIP1} (SC-1641), p16^{INK4a} (SC-759), p53 (SC-6243), actin (SC-1616), HA tag (SC-7392), and Cdc20 (SC-5269) antibodies from Santa Cruz Biotechnology, Inc., Santa Cruz, CA, USA; the Cdh1 antibody from Oncogene, Inc. (CC43), the Flag antibody from Sigma (F3165); the Skp2 antibody (32-3400) from Zymed; and the pRB antibody from BD Pharmingen (#554136). The antibody against human securin was generously provided by Hui Zou of the UT Southwestern Medical School.

Production of lentivirus vectors

Lentivirus vectors were produced by transient transfection of HEK293T cells using a calcium phosphate transfection kit (Invitrogen Life Technologies, Carlsbad, CA). The vector plasmid (10 µg) HR'CMV-Tax together with two packaging plasmids, pCMVΔ8.2ΔVpr (vpr-null, env-null, 10 µg) and pCMV-VSV-G (vesicular stomatitis virus G-glycoprotein, 2 µg), were used to transfect 5 × 10⁶ 293T cells that had been plated in a T75 flask 1 day before. The calcium phosphate/DNA precipitate was added to cells in complete DMEM medium. After 16 h, cells were washed with 5 ml PBS to remove the DNA, and incubated in 5 ml complete DMEM. Vector supernatants were collected at 24 and 48 h post-transfection. The supernatant was centrifuged at low speed to remove cellular debris and concentrated by ultracentrifugation in a Beckman SW28 rotor at 24 000 r.p.m. for 2 h at 4°C. The vector-enriched pellet was resuspended in DMEM and aliquoted for storage at -80°C. Vector stocks were normalized by p24-Gag content measured with an enzyme-linked immunosorbent assay (Beckman-Coulter) and titered by immunofluorescence or visualization of GFP after gene transduction.

Cell cycle synchronization and infection by lentivirus or adenovirus vectors

Cell cycle synchronization and infection of synchronized HeLa cells with adenovirus vectors were as reported previously (Liu *et al.*, 2003). Infection with lentiviral vectors was carried out 1 h after release from the G₁/S arrest.

Senescence-associated β-galactosidase (SA β-Gal) staining

HeLa cells (2.5 × 10⁴/well) in monolayer were grown in a six-well plate, transduced with LV-Tax or LV-GFP at an m.o.i. of 5, grown for 3 days, washed in 2 ml PBS, fixed for 3–5 min at room temperature in 2 ml of a solution containing 2% formaldehyde, 0.2% glutaraldehyde (or 3% formaldehyde), washed, and incubated for 24 h at 37°C with a solution (3 ml) containing 1 mg/ml of 5-bromo-4-chloro-3-indolyl β-D-galactoside (X-Gal), 40 mM citric acid/sodium

phosphate at pH 6.0, 5 mM potassium ferrocyanide, 5 mM potassium ferricyanide, 150 mM NaCl, and 2 mM MgCl₂.

Detection of Skp2 polyubiquitination in asynchronous HeLa cells

Two hundred thousand HeLa cells were grown in a 10 cm Petri dish and transfected with 10 µg each of an expression plasmid for the FLAG-tagged human Skp2 and that for the HA-tagged human ubiquitin (HA-Ub) using the FuGENE 6 transfection reagents (Roche Applied Science). The second day, cells were infected with Ad-Tax or Ad-tTa at an m.o.i. of 5 for 16 h, and then treated with 10 µM MG132 for 4 h. Cells were lysed in RIPA buffer (50 mM Tris, 150 mM NaCl, 0.5% DOC, 1% NP-40, 0.1% SDS) containing 1 × protease inhibition cocktail (Roche Applied Science) and immunoprecipitated with a mouse monoclonal Flag antibody (F3165, Sigma, Inc. USA) at 4°C overnight. The immunoprecipitates were washed three times with PBS and immunoblotted with a mouse anti-HA antibody (SC-7392, Santa Cruz).

Detection of Skp2 polyubiquitination in synchronized HeLa cells

HeLa cells were transfected similarly as above. At 4 h after transfection, cells were subjected synchronized by DTB. Throughout the duration of the second thymidine treatment, cells were infected with Ad-Tax or Ad-tTa at an m.o.i. of 5. The cells were then released into complete medium containing 10 µM MG132, and harvested at the indicated times (0, 4, 5, 6, 7, and 8 h) post-release for immunoprecipitation and immunoblots.

Quantitative real-time PCR

HeLa cells were transduced with LV-Tax or LV-GFP for 3 days. Cells were harvested and total cellular RNA was isolated using the Trizol reagent (Invitrogen). The amount of total RNA in each sample was estimated based on the levels of 28S, 18S, and 5S rRNAs resolved in native 1% agarose gels. The first-strand cDNA synthesis was carried out with a kit from Amersham Biosciences according to the manufacturer's protocol. The cDNA samples were then stored frozen at -80°C. The real-time PCR for p21^{CIP1/WAF1}, p27^{KIP1}, and the internal β-actin control were performed using the universal master mix and kits from the Applied Biosystems (part number 4331182), which consist of gene-specific TagMan MGB probes (6-FAMTM dye-labeled) and unlabeled PCR primer pairs for p21^{CIP1/WAF1} (Hs003555782_m1, CDKN1A), p27^{KIP1} (Hs00153277_m1, CDKN1B), and β-actin (Hs99999903_m1, ActB), respectively. Each real-time PCR reaction contained the first-strand cDNA, the respective primer pair, and the gene-specific TagMan MGB probe, and was carried out in an ABI Prism 7000 Sequence Detection System. The PCR condition was 95°C for 10 min, followed by 95°C for 15 s, and 60°C for 1 min in each cycle, for 40 cycles. Four concentrations (successive four-fold dilution) of the first-strand cDNA were analyzed to establish linearity of the real-time PCR. The levels of p21^{CIP1/WAF1} and p27^{KIP1} mRNA in either LV-Tax/HeLa or LV-GFP/HeLa sample were normalized against that of the β-actin. The fold increases of p21^{CIP1/WAF1} and p27^{KIP1} mRNA in LV-Tax/HeLa versus LV-GFP/HeLa were calculated and plotted. Similarly, RT-PCR was used to measure p21^{CIP1/WAF1}, p27^{KIP1}, and Skp2 mRNA levels using the level of 18S ribosomal RNA as an internal control. The PCR primer pairs for Skp2 and 18S RNA were (Hs00180634_m1, Skp2) and (Hs99999901_s1, 18S), respectively. The levels of p21^{CIP1/WAF1}, p27^{KIP1} and Skp2 mRNA in HTLV-transformed T cells and HTLV-1-unrelated CEM, Jurkat, and SupT1T cells were normalized against that of the 18S RNA first. The ratios of p21^{CIP1/WAF1}, p27^{KIP1}, and Skp2 mRNA of Jurkat versus the other T cells were then computed. The RT-PCR for Ad-Tax- and Ad-tTa-transduced cells was carried out similarly.

Pulse chase for p27^{KIP1}

HeLa cells were transduced with LV-Tax or LV-GFP for 3 days. One hundred thousand cells from each transduction were washed with 10 ml warm PBS twice to remove methionine and cysteine. The cells were then trypsinized and resuspended in 10 ml warm PBS, spun down, and resuspended in 1 ml methionine-free, cysteine-free DME complete medium containing 2% dialyzed FBS. The cells were starved for methionine and cysteine for 20 min at 37°C, thereupon, 560 µCi of promix L-S35 (14.3 µCi/µl, AGQ0080, Amersham Biosciences, Piscataway, NJ, USA) containing L-S³⁵-methionine and L-S³⁵-cysteine was added and the cells were pulse-labeled for

1 h. Radiolabeled cells were spun down and the radioactive media removed. The cells were then washed with 5 ml of warm PBS, transferred to 4 ml of a chase medium composed of DME complete medium supplemented with 10% FBS and 2 mM each of methionine and cysteine. Aliquot of cells (1 ml) was then taken at the indicated time points (0, 1, 3, and 6 h), harvested, lysed, and immunoprecipitated using a p27^{KIP1} antibody (SC-528, Santa Cruz).

siRNA knockdown of Cdc20 and Cdh1

Two hundred thousand HeLa cells were seeded in each well of six-well plates and synchronized by double thymidine treatment as described above. At 2 h before the second thymidine treatment, cells were transfected with 120 pmol of a control siRNA, a Cdc20 siRNA, a Cdh1 siRNA, or a combination of both Cdc20 and Cdh1 siRNAs. Transfections were carried out using oligofectamine (Invitrogen, Inc.) as prescribed by the manufacturer. After 4 h into the second thymidine treatment, cells were infected with either Ad-Tax or Ad-tTa (m.o.i. = 5). The infection was carried out for the duration

of the remainder of the second thymidine treatment for 12 h. Cells were then released from the arrest and collected at 8 h after release for immunoblots. The siRNA oligonucleotides, control nontargeting siRNA (Cat No: D-001210-01-20), Cdc20 siRNA (p55CDC, human, Cat No: M-003225-03), and Cdh1 siRNA (CDH1, human, Cat No: M-015377-01), were purchased from Dharmacon Inc.

Acknowledgements

We thank M Pagano for the Flag-Skp2 plasmid, Dr S Hatakeyama for the HA-ubiquitin expression plasmid, ISY Chen, PM Cannon, and I Christodouloupoulos for lentiviral vectors, Andrew Koff for wild-type, p21-null, and p27-null NIH3T3 cells, H Zou for the human securin antibody, G Franchini, H Yu, K Lee, T Dunn, and O Cohen-Fix for helpful discussions, and X Xiang and P Grimley for critical reading of the manuscript. This work was supported by grants from the National Institutes of Health to C-ZG.

References

- Akagi T, Ono H, Shimotohno K (1996) Expression of cell-cycle regulatory genes in HTLV-I infected T-cell lines: possible involvement of Tax1 in the altered expression of cyclin D2, p18Ink4 and p21Waf1/Cip1/Sdi1. *Oncogene* **12**: 1645–1652
- Bashir T, Dorrello NV, Amador V, Guardavaccaro D, Pagano M (2004) Control of the SCF(Skp2-Cks1) ubiquitin ligase by the APC/C(Cdh1) ubiquitin ligase. *Nature* **428**: 190–193
- Bornstein G, Bloom J, Sitry-Shevah D, Nakayama K, Pagano M, Hershko A (2003) Role of the SCFSkp2 ubiquitin ligase in the degradation of p21Cip1 in S phase. *J Biol Chem* **278**: 25752–25757
- Carrano AC, Eytan E, Hershko A, Pagano M (1999) SKP2 is required for ubiquitin-mediated degradation of the CDK inhibitor p27. *Nat Cell Biol* **1**: 193–199
- Cereseto A, Washington PR, Rivadeneira E, Franchini G (1999) Limiting amounts of p27Kip1 correlates with constitutive activation of cyclin E-CDK2 complex in HTLV-I-transformed T-cells. *Oncogene* **18**: 2441–2450
- Chang BD, Broude EV, Dokmanovic M, Zhu H, Ruth A, Xuan Y, Kandel ES, Lausch E, Christov K, Roninson IB (1999) A senescence-like phenotype distinguishes tumor cells that undergo terminal proliferation arrest after exposure to anticancer agents. *Cancer Res* **59**: 3761–3767
- Chin L, Artandi SE, Shen Q, Tam A, Lee SL, Gottlieb GJ, Greider CW, DePinho RA (1999) p53 deficiency rescues the adverse effects of telomere loss and cooperates with telomere dysfunction to accelerate carcinogenesis. *Cell* **97**: 527–538
- Chowdhury IH, Farhadi A, Wang XF, Robb ML, Birs DL, Kim JH (2003) Human T-cell leukemia virus type 1 Tax activates cyclin-dependent kinase inhibitor p21/Waf1/Cip1 expression through a p53-independent mechanism: inhibition of cdk2. *Int J Cancer* **107**: 603–611
- Chu ZL, Di Donato JA, Hawiger J, Ballard DW (1998) The tax oncoprotein of human T-cell leukemia virus type 1 associates with and persistently activates IκappaB kinases containing IKKalpha and IKKbeta. *J Biol Chem* **273**: 15891–15894
- de la Fuente C, Wang L, Wang D, Deng L, Wu K, Li H, Stein LD, Denny T, Coffman F, Kehn K, Baylor S, Maddukuri A, Pumfery A, Kashanchi F (2003) Paradoxical effects of a stress signal on pro- and anti-apoptotic machinery in HTLV-1 Tax expressing cells. *Mol Cell Biochem* **245**: 99–113
- Dimri GP, Lee X, Basile G, Acosta M, Scott G, Roskelley C, Medrano EE, Linskens M, Rubelj I, Pereira-Smith O (1995) A biomarker that identifies senescent human cells in culture and in aging skin *in vivo*. *Proc Natl Acad Sci USA* **92**: 9363–9367
- Ferbeyre G, de Stanchina E, Lin AW, Querido E, McCurrach ME, Hannon GJ, Lowe SW (2002) Oncogenic ras and p53 cooperate to induce cellular senescence. *Mol Cell Biol* **22**: 3497–3508
- Franchini G, Wong-Staal F, Gallo RC (1984) Human T-cell leukemia virus (HTLV-I) transcripts in fresh and cultured cells of patients with adult T-cell leukemia. *Proc Natl Acad Sci USA* **81**: 6207–6211
- Fu DX, Kuo YL, Liu B, Jeang KT, Giam CZ (2003) Human T-lymphotropic virus type I tax activates I-kappa B kinase by inhibiting I-kappa B kinase-associated serine/threonine protein phosphatase 2A. *J Biol Chem* **278**: 1487–1493
- Ganoth D, Bornstein G, Ko TK, Larsen B, Tyers M, Pagano M, Hershko A (2001) The cell-cycle regulatory protein Cks1 is required for SCF(Skp2)-mediated ubiquitinylation of p27. *Nat Cell Biol* **3**: 321–324
- Hara T, Kamura T, Nakayama K, Oshikawa K, Hatakeyama S, Nakayama K (2001) Degradation of p27(Kip1) at the G(0)-G(1) transition mediated by a Skp2-independent ubiquitination pathway. *J Biol Chem* **276**: 48937–48943
- Helt AM, Galloway DA (2003) Mechanisms by which DNA tumor virus oncoproteins target the Rb family of pocket proteins. *Carcinogenesis* **24**: 159–169
- Jeang KT, Giam CZ, Majone F, Aboud M (2004) Life, death, and tax: role of HTLV-I oncoprotein in genetic instability and cellular transformation. *J Biol Chem* **279**: 31991–31994
- Jin DY, Giordano V, Kibler KV, Nakano H, Jeang KT (1999) Role of adapter function in oncoprotein-mediated activation of NF-kappaB. Human T-cell leukemia virus type I Tax interacts directly with IκappaB kinase gamma. *J Biol Chem* **274**: 17402–17405
- Kawata S, Ariumi Y, Shimotohno K (2003) p21(Waf1/Cip1/Sdi1) prevents apoptosis as well as stimulates growth in cells transformed or immortalized by human T-cell leukemia virus type 1-encoded tax. *J Virol* **77**: 7291–7299
- Korber B, Okayama A, Donnelly R, Tachibana N, Essex M (1991) Polymerase chain reaction analysis of defective human T-cell leukemia virus type I proviral genomes in leukemic cells of patients with adult T-cell leukemia. *J Virol* **65**: 5471–5476
- Liang MH, Geisbert T, Yao Y, Hinrichs SH, Giam CZ (2002) Human T-lymphotropic virus type 1 oncoprotein tax promotes S-phase entry but blocks mitosis. *J Virol* **76**: 4022–4033
- Lim MS, Adamson A, Lin Z, Perez-Ordóñez B, Jordan RC, Tripp S, Perkins SL, Elenitoba-Johnson KS (2002) Expression of Skp2, a p27(Kip1) ubiquitin ligase, in malignant lymphoma: correlation with p27(Kip1) and proliferation index. *Blood* **100**: 2950–2956
- Liu B, Hong S, Tang Z, Yu H, Giam CZ (2005) HTLV-I Tax directly binds the Cdc20-associated anaphase-promoting complex and activates it ahead of schedule. *Proc Natl Acad Sci USA* **102**: 63–68
- Liu B, Liang MH, Kuo YL, Liao W, Boros I, Kleinberger T, Blancato J, Giam CZ (2003) Human T-lymphotropic virus type 1 oncoprotein tax promotes unscheduled degradation of Pds1p/securin and Clb2p/cyclin B1 and causes chromosomal instability. *Mol Cell Biol* **23**: 5269–5281
- Nakayama K, Nagahama H, Minamishima YA, Matsumoto M, Nakamichi I, Kitagawa K, Shirane M, Tsunematsu R, Tsukiyama T, Ishida N, Kitagawa M, Nakayama K, Hatakeyama S (2000) Targeted disruption of Skp2 results in accumulation of cyclin E and p27(Kip1), polyploidy and centrosome overduplication. *EMBO J* **19**: 2069–2081
- Nakayama K, Nagahama H, Minamishima YA, Miyake S, Ishida N, Hatakeyama S, Kitagawa M, Iemura S, Natsume T, Nakayama KI (2004) Skp2-mediated degradation of p27 regulates progression into mitosis. *Dev Cell* **6**: 661–672
- Naldini L, Blomer U, Gallay P, Ory D, Mulligan R, Gage FH, Verma IM, Trono D (1996) *In vivo* gene delivery and stable transduction of nondividing cells by a lentiviral vector. *Science* **272**: 263–267

- Scheffner M, Werness BA, Huibregtse JM, Levine AJ, Howley PM (1990) The E6 oncoprotein encoded by human papillomavirus types 16 and 18 promotes the degradation of p53. *Cell* **63**: 1129–1136
- Serrano M, Lin AW, McCurrach ME, Beach D, Lowe SW (1997) Oncogenic ras provokes premature cell senescence associated with accumulation of p53 and p16INK4a. *Cell* **88**: 593–602
- Sun SC, Ballard DW (1999) Persistent activation of NF-kappaB by the tax transforming protein of HTLV-1: hijacking cellular IkappaB kinases. *Oncogene* **18**: 6948–6958
- Swanson C, Ross J, Jackson PK (2000) Nuclear accumulation of cyclin E/Cdk2 triggers a concentration-dependent switch for the destruction of p27Xic1. *Proc Natl Acad Sci USA* **97**: 7796–7801
- Wei W, Ayad NG, Wan Y, Zhang GJ, Kirschner MW, Kaelin Jr WG (2004) Degradation of the SCF component Skp2 in cell-cycle phase G1 by the anaphase-promoting complex. *Nature* **428**: 194–198
- Wells SI, Aronow BJ, Wise TM, Williams SS, Couget JA, Howley PM (2003) Transcriptome signature of irreversible senescence in human papillomavirus-positive cervical cancer cells. *Proc Natl Acad Sci USA* **100**: 7093–7098
- Wells SI, Francis DA, Karpova AY, Dowhanick JJ, Benson JD, Howley PM (2000) Papillomavirus E2 induces senescence in HPV-positive cells via pRB- and p21(CIP)-dependent pathways. *EMBO J* **19**: 5762–5771
- Xiao G, Sun SC (2000) Activation of IKKalpha and IKKbeta through their fusion with HTLV-I tax protein. *Oncogene* **19**: 5198–5203
- Yamaoka S, Courtois G, Bessia C, Whiteside ST, Weil R, Agou F, Kirk HE, Kay RJ, Israel A (1998) Complementation cloning of NEMO, a component of the IkappaB kinase complex essential for NF-kappaB activation. *Cell* **93**: 1231–1240
- Zhu XH, Nguyen H, Halicka HD, Traganos F, Koff A (2004) Noncatalytic requirement for cyclin A-cdk2 in p27 turnover. *Mol Cell Biol* **24**: 6058–6066